Title

Functional Organic Semiconductors Based on Bay-Annulated Indigo (BAI)

Journal

The Chemical Record, 19(6)

ISSN

1527-8999

Authors

Kolaczkowski, Matthew A

Liu, Yi

Publication Date

2019-06-01

DOI

10.1002/tcr.201800159

Peer reviewed

Personal Account

THE CHEMICAL RECORD

DOI: 10.1002/tcr.201800159

Functional Organic Semiconductors Based on Bay-Annulated Indigo (BAI)

Matthew A. Kolaczkowski[a, b] and Yi Liu*[a]

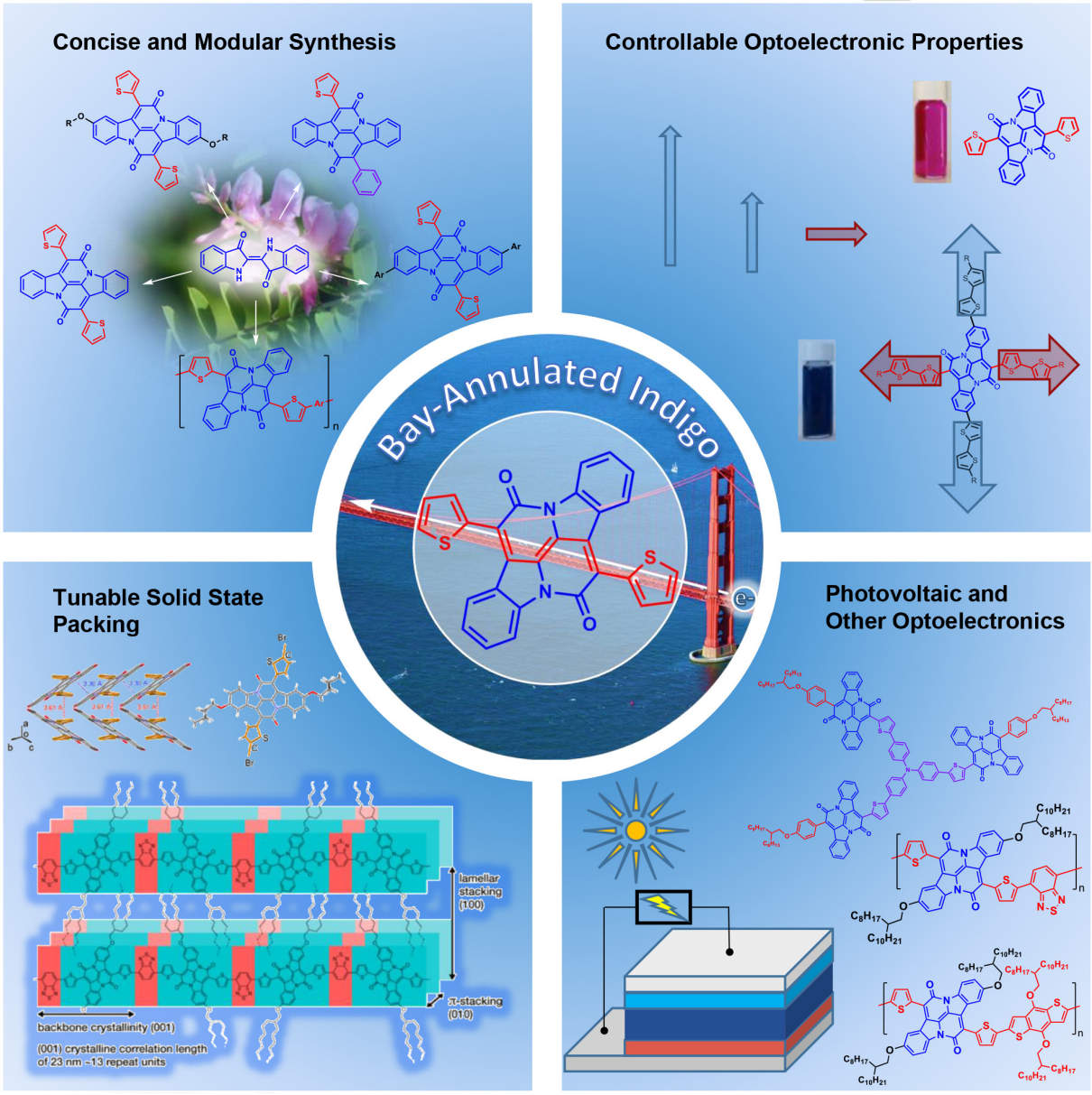

Abstract: The advancement of organic electronics has been continually pushed by the need for stable and high performance acceptor materials. By utilizing inexpensive and stable indigo dye as a starting material, Bay-Annulated Indigo (BAI) provides a new motif for the development of semiconducting materials. Modular and straightforward synthesis makes BAI an outstanding platform for molecular design, while excellent stability, strong absorption, and high ambipolar mobility render BAI-based materials excellent candidates for organic electronics. BAI-based polymers and small molecules have taken advantage of these properties to show promising results in a variety of applications.

Keywords: Bay-Annulated Indigo, Electron Acceptor, Indigo, Organic Photovoltaics, Panchromatic Absorption

1. Introduction

Evolution in material synthesis and device structure has brought the field of organic electronics ever closer to the goal of inexpensive, printable electronics. A fully realized organic electronics field holds the temptation of biologically compatible devices, light-weight solar cells that could be inexpensively printed onto flexible substrates, smart windows, and a myriad of other applications.[1] Despite these advances, the availability of high-performance materials still remains one of the largest barriers between those dreams and reality.

Ideal organic semiconducting materials would be stable, conjugated to allow for the flow of charges and high carrier mobilities, good light absorbers, planar to encourage favorable arrangement with other components, and easy to process into devices. There are a number of strategies in order to fulfill these requirements, but the most utilized and consistent are "push-pull" systems.[2] By alternating electron rich and electron poor building blocks, these molecules and polymers are able to absorb a greater portion of the light spectrum and the energetics of the system can be controlled, making it possible to improve the semiconducting properties.

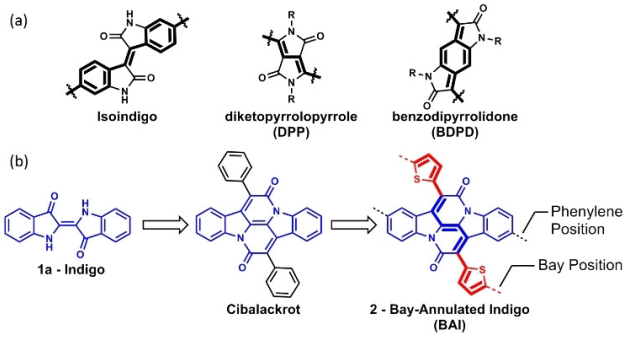

Figure 1. (a) Examples of common amide-based acceptor monomers with conjugation pathway accentuated with bolded bonds (b) Introduction of conjugation pathway in BAI via annulation of the parent indigo.

[a] *M. A. Kolaczkowski, Dr. Y. Liu*
The Molecular Foundry
Lawrence Berkeley National Laboratory
One Cyclotron Road
Berkeley, CA 94720, United States
E-mail: yliu@lbl.gov
[b] *M. A. Kolaczkowski*
College of Chemistry
University of California, Berkeley
Berkeley, CA 94720, United States

While there are a wide variety of high performing electron donating building blocks available, electron deficient units are comparatively underdeveloped. Amide groups, perhaps best known for making up the backbone of proteins, are great candidates for building robust acceptor materials. A number of established amide-based acceptors such as isoindigo, diketopyrrolopyrrole (DPP),[3] and benzodipyrrolidone (BPDP), have already pushed the boundaries of the field (Figure 1 a).[4] In addition to the coplanarity, these systems also feature the attachment of two strongly withdrawing amide groups immediately next to the conjugation pathway (visualized through bolded bonds).

We were particularly taken by indigo **1** with its outstanding stability, rich history, and global presence (Figure 1 b). Widely known as the molecule responsible for the color of blue jeans, this dye has been utilized for over 6000 years and is produced at over 50 kilotons per year.[5] The functional-group rich molecule contains a C=C double bond, two amine groups and two carbonyl groups, which at the same time maintain high planarity due to intramolecular hydrogen bonding interactions. A vinylogous amide in its own right, it is astounding that a molecule of such small size is capable of absorbing light into the red region of the visible spectrum.[6] It has been utilized in limited organic electronics applications, showing good stability and the ability to conduct both electrons and holes efficiently. However, one of the properties that makes indigo a fantastic dye, namely its low solubility, renders it highly impractical to process into devices. Vacuum deposition and protection-deprotection routes have been utilized, but have also encountered issues with scalability and morphological defects.[7]

In order to make indigo into a higher performing and processable material there are a number of functional handles available. Unfortunately, individual modification of the

amine, ketone, and phenyl groups do not allow for uninterrupted conjugation through the molecule, a necessity for polymeric systems. Cibalackrot, an indigo-derived dye first produced by The Swiss Society of Chemical Industry of Basle (CIBA) in 1914, provided a creative solution to these problems (Figure 1 b).[8]

By combining *N*-alkylation and carbonyl condensation at the "bay positions" of Indigo, the coplanarity of the parent indigo is reinforced after replacing the intramolecular H-bonding groups with two annulated rings.

Furthermore, this annulation opens up an uninterrupted conjugation pathway that is orthogonal to the long molecular axis of the parent indigo molecule, concurrent with two amide groups installed adjacent to the conjugation pathway. These features endowed excellent electron accepting characteristics for Cibalackrot, yet its use in organic semiconductors had not been explored until 2014. By altering the phenyl groups with the more electron-donating thiophene groups, the parent Bay-Annulated Indigo (BAI) **2** was first conceived and has been subsequently shown to behave as a versatile electron accepting unit for a wide variety of molecules and polymers with a diverse set of properties.[9] Herein, we summarize efforts made by our group and others to advance the BAI moiety in synthesis and organic electronics applications, with a focus on photovoltaics.

2. Production and Properties

2.1. Synthesis

Because of the abundance of indigo, the starting material for synthesizing BAI can be obtained inexpensively (several US dollars per kilogram). Simple treatment of indigo with commercially available 2-thiopheneacetyl chloride (4 equivalents) under refluxing xylene conditions provides good yields of the BAI product which can be purified in gram scales by precipitation (Figure 2).[9] A proposed mechanism involves initial condensation of the indigo amine with thiopheneacetyl chloride followed by quick condensation of the activated methylene position onto the carbonyl (attempts at isolating the pre-ring closed product were unsuccessful).

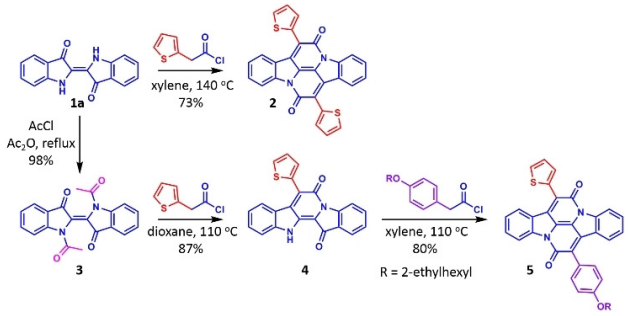

Figure 2. Indigo annulation reactions forming both symmetric BAI compounds **2**, or utilizing diacetylindigo **3** as a soluble precursor for the formation of monoannulated **4** and desymmetrized BAI **5**.

Because an equivalent of water is formed during the condensation step, an equivalent amount of thiopheneacetyl chloride is made inactive due to hydrolysis. To combat this, a modified protocol involving the pretreatment of indigo with acetyl chloride was developed. In this scenario, water that forms in the condensation can deacylate indigo, forming an equivalent of acetic acid which is significantly less nucleophilic than water, slowing degradation of the thiopheneacetyl chloride reagent. Reaction between acetic acid and the thiopheneacetyl chloride would form a mixed anhydride which is still a competent intermediate for this reaction. The

Matthew Kolaczkowski received his B.S. in chemistry at the University of Illinois at Urbana-Champaign in 2013. He is currently a Ph.D. candidate in synthetic organic chemistry at the University of California, Berkeley. His current research focuses on the design and synthesis of organic semiconducting small molecules and polymers under the supervision of Dr. Yi Liu at Lawrence Berkeley National Laboratory.

Yi Liu is a Career Staff Scientist at the Molecular Foundry, Lawrence Berkeley National Laboratory, USA. He obtained his Ph.D. degree in Chemistry in 2004 from the University of California, Los Angeles. After his post-doctoral research at the Scripps Research Institute, he joined the Molecular Foundry in 2006 as an independent principal investigator. His research interests include design and self-assembly of functional organic and organic-inorganic hybrid framework materials, materials chemistry for organic electronics, and fundamental understanding of the associated electronic processes.

result is an annulation reaction that allows for clean conversion to a single addition product **4** with only 1 equivalent of thiopheneacetyl chloride needed. Initial deacylation of **1a** is proposed to come from a catalytic amount of water. The *N*-acetylation also transforms the parent indigo into a highly soluble species that permits simple monitoring of the reaction progress. As a result, annulation on the two bay positions can be conducted stepwise with two different aromatic-acetyl chlorides, opening the door for dissymmetrically functionalized BAI derivatives, such as **5**.[10] This differential substitution allows for the design of molecules capable of supramolecular assembly such as the amphiphilic BAI **6** (Figure 5). BAI oligomers, such as **7** and **8** can also be synthesized through this route. An interesting example is triphenylamine based compound **9**, which has a C_3 symmetric structure that can spontaneously self-assembly into nanowires.

The BAI core can be further expanded from the phenylene positions by starting with functionalized indigo derivatives, although these precursors are less readily available and more expensive. These are most often produced at lab scale through the Baeyer-Drewsen synthesis from the commercially available substituted nitrobenzaldehydes (Figure 3).[11] Alkyl ether derivatives are particularly handy for increasing solubility while bromide substitution provides a convenient functional handle for further cross coupling reactions.

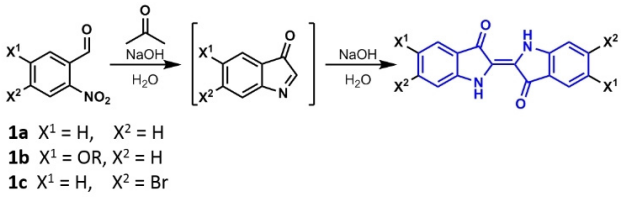

Figure 3. Generalized Baeyer-Drewsen synthesis of indigos with relevant substitution patterns. Parent indigo **1**, 5,5'-dihydroxy or alkyoxy indigo **1b**, and 6,6'-dibromoindigo **1c** can be produced with this method.

Various aromatic groups can be coupled to 6,6'-dibromo functionalized BAI through transition metal catalyzed Stille and Suzuki cross-couplings (Figure 4). Thienyl rings at the bay position can be selectively brominated at the 2-position, opening up another avenue for derivatization.[12] BAI can also be used as a monomer for the synthesis of conjugated polymers, which have been accomplished primarily through Stille coupling.

While the hydrogen bonding of indigo is removed in the formation of BAI, strong π-π stacking induced aggregation was observed due to its reinforced coplanarity, resulting in low solubility species. Because solution processing is crucial

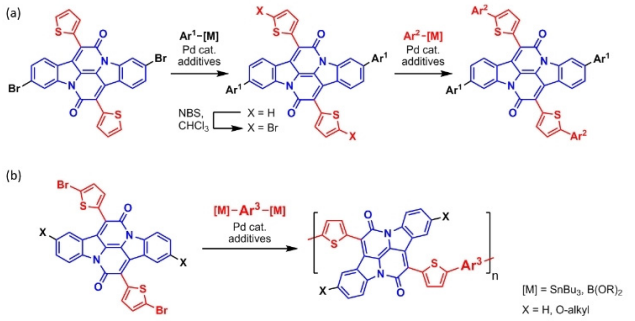

Figure 4. Functionalization of the BAI core. (a) Bay-annulation of **1c** allows for arylation at the 6,6' position. Bromination of the phenylene position allows for further derivatization to give small molecules or (b) polymers.

to the success of these materials, solubilizing groups are often incorporated to improve solubility. However, addition of excessively large alkyl chains adds an insulating layer between compounds, potentially decreasing conductivity. Because of this balance between solubility and conductivity many sites and types of solubilizing groups have been utilized.[13] By using 5,5'-dihydroxy or dialkoxy prefunctionalized indigo, a number of alkyl chains can be added to the phenyl groups before bay-annulation (Figure 5 a). These are often branched to increase solubility, but a sizable variety of sidechains have been explored and demonstrated, such as in compounds **10**, **11**, **12**, **13**.[14] In addition, BAI derivatives made from 6,6'-dibromoindigo can cross couple with aromatic groups with pre-attached alkyl chains which both increase solubility and overall π-surface area, a method utilized for compounds **14–17** and polymers in Figure 6. An alternative strategy is to perform the annulation reaction with pre-alkylated thiopheneacetyl or phenylacetyl chlorides, as shown by compounds **18** through **21**.[10] This method is used to provide amphiphilic properties to **6** through installation of both a water soluble glycol chain and a hydrophobic 2-ethylhexyl sidechain. It is worth noting that although BAI is only a fraction of the overall structure which can be fairly complex and expensive to make, the ready availability of BAI provides an easy access to a more extensive material set.

2.2. Solid-State Behavior

Morphological control of these materials in the solid state is crucial for their use in thin-film devices. Use of Grazing Incidence Wide Angle X-ray Spectroscopy (GIWAXS) has provided great insight into the order of BAI-based polymers in the solid state. A spuncast film of polymer **P1** displays (100) and (200) peaks in the q_z axis, indicating an edge-on lamellar orientation (Figure 7).[9] When annealing at 250 °C, peak narrowing and emergence of the (300) peak indicates an increased crystallinity in the lamellar edge-on orientation. In

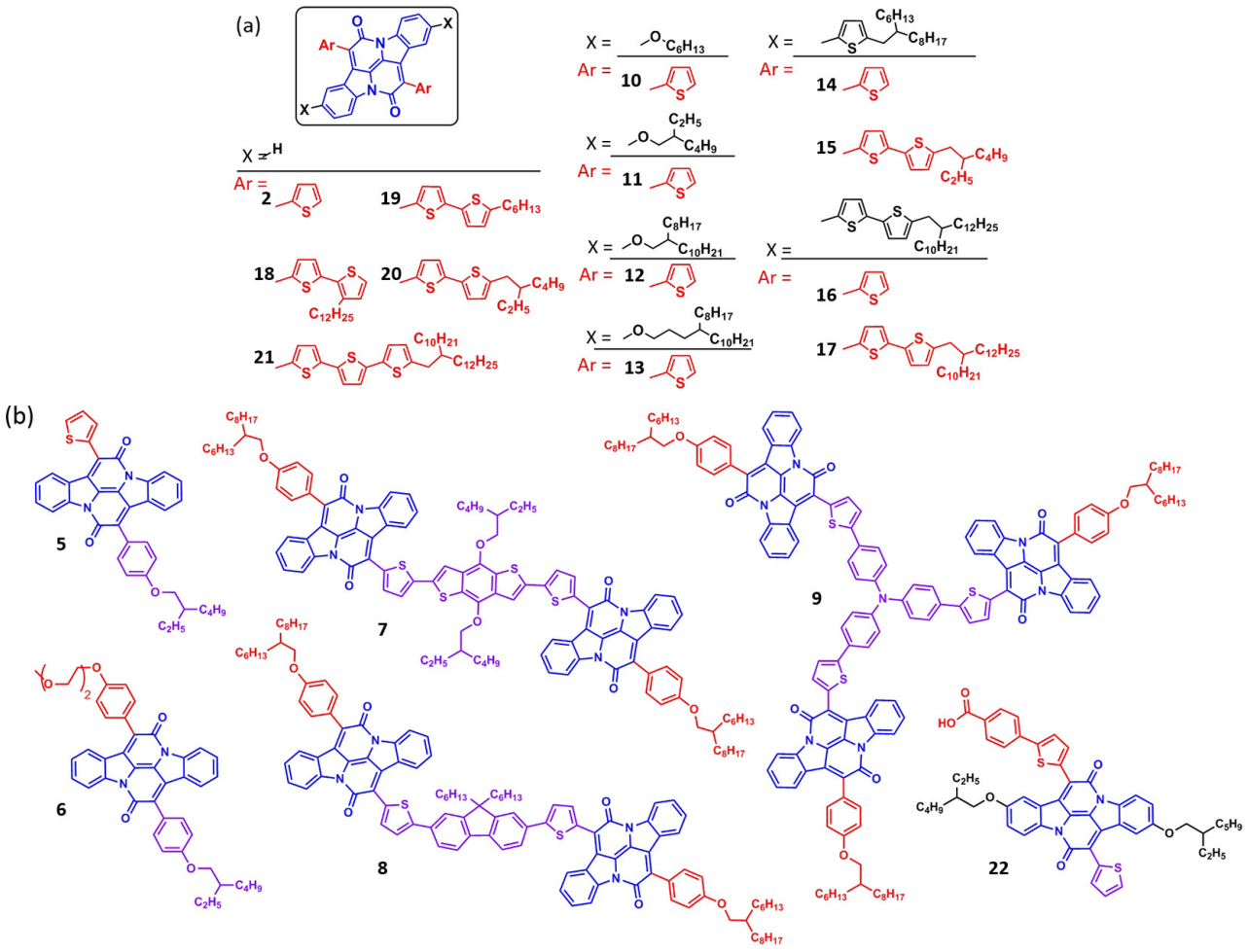

Figure 5. List of reported a) symmetric and b) dissymmetric BAI small molecules. The BAI core is colored in blue with phenylene substitution in black (X=), and bay substitution in red (Ar=), and secondary bay substitution in purple.

addition, a defined (010) reflection in the q_{xy} plane provides further evidence for an edge-on orientation with a π-π stacking distance of 3.83 Å. Depending on the monomer chosen, it is fairly common for BAI containing polymers to take on a mixed edge-on and face-on orientation as well. This is especially the case for polymers with long alkyl chains such as **P15–P18**.

P14 displays this slightly mixed edge-on/face-on morphology.[15] In addition to a crystalline lamellar stacking indicated by the out-of-plane (n00) (n up to 4) stacking, its GIWAXS pattern also shows a striking (001) peak, corresponding to backbone ordering to the length of 23 nm, equivalent to 13 repeat units on average (Figure 8). Moving the branching point of the sidechain further from the polymer backbone increases the unit cell size (100) while allowing closer packing between polymer chains (010). The effect of alkyl chain appears to have very little effect on the backbone crystallinity (001) reflection, pointing to a substantial driving force for maintaining backbone conjugation.

Interestingly, despite the long range polymer backbone order found from GIWAXS, a single crystal x-ray crystal structure of the monomeric species shows that the thiophene rings in the Bay position are not planar (Figure 9 a).[16]

Computational analysis comparing the energetics of bond angle rotation of **12** and naphthylenediimide with a pendant thiophene (**NDI-T**) give some interesting insights. The Bay thiophene rotation angle shows high barriers to both planarity ($\Delta^{\circ}=0^{\circ}$) due to steric S–O and H–O interactions but also to perpendicular orientation to the BAI core ($\Delta^{\circ}=90^{\circ}$) due to loss of electronic conjugation (Figure 9 b).[15] Although not planar, these two barriers effectively lock the BAI thiophene into a 30° angle with respect to the BAI core, allowing some level of conformational flexibility while maintaining effective conjugation. These combined factors explain the consistently

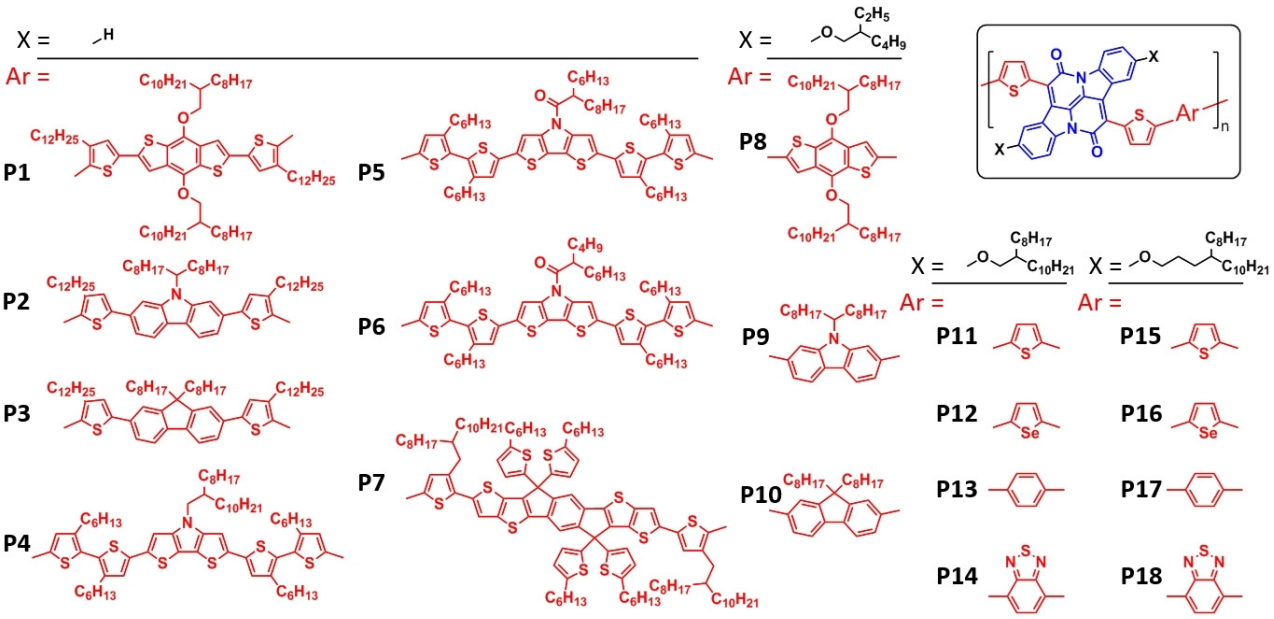

Figure 6. List of reported BAI polymers. The BAI core is colored in blue with phenylene substitution in black (X=), and bay substitution in red (Ar=).

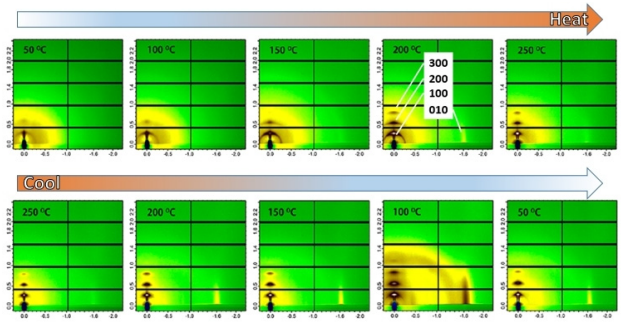

Figure 7. Variable temperature GIWAXS of **P1** showing the thermally induced crystallinity changes. Reproduced with permission from reference [9], Copyright © 2014, American Chemical Society.

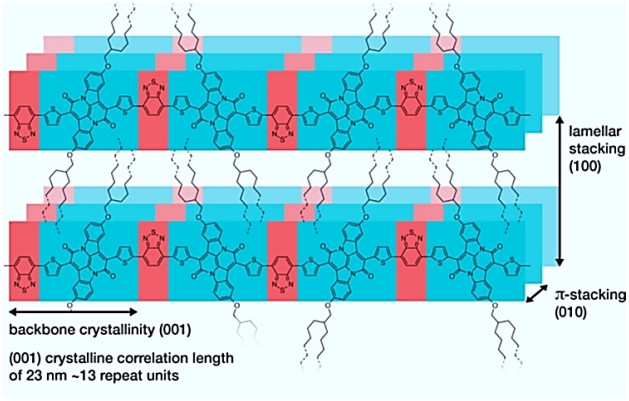

Figure 8. Illustration of the packing structure of **P14** based on GIWAXS analysis. Reproduced with permission from reference [15], Copyright © 2016, American Chemical Society.

large correlation lengths of BAI polymer backbones as well as their impressive conductivity despite non-planarity.

2.3. Optoelectronic Properties

Due to the extended conjugation and donor-acceptor nature of BAI **2**, these molecules absorb light into the visible spectrum and near-IR (Figure 10a).

The characteristic donor-acceptor peaks corresponding to electronic π-π* and intramolecular charge transfer processes occur at the longest wavelengths. This often appears as an initial broad π-π* peak with a shoulder attributed to charge-transfer processes.

As conjugation is extended along the Bay position as in **20**, the absorption peak is red-shifted due to both larger conjugation area and stronger donor character paired with the BAI acceptor (Figure 10b). Absorption to 1000 nm or above is facilitated by more electron rich donor monomers. The extinction coefficients of polymers regularly reach $\varepsilon = 10^5$ whereas small molecules generally exhibit coefficients in the $\varepsilon = 10^4$ range.

While extended conjugation in the Bay direction pushes the absorption to longer wavelengths, it leaves a large void space in the blue region of the visible spectrum.[17] Interestingly, by extending conjugation off of the phenylene position

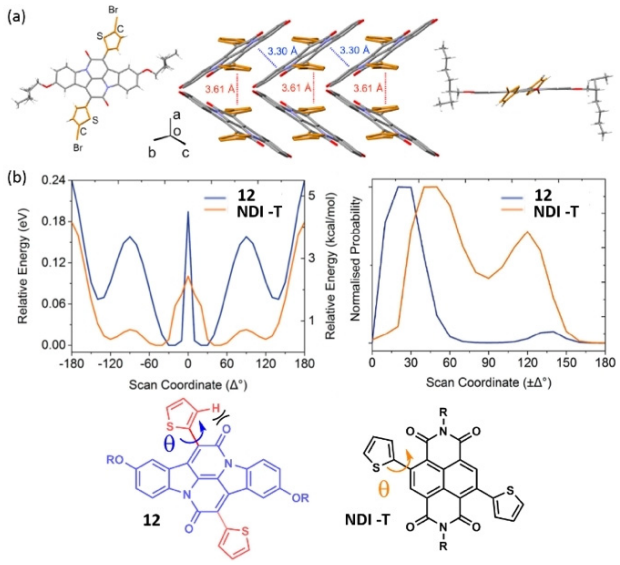

Figure 9. Analysis of bay position bond angle θ through (a) crystal structure and (b) computational bond angle analysis comparing the bond energetics and Boltzmann probability distribution of rotational conformations between BAI **12** (blue) and **NDI-T** (orange). Reproduced with permission from references [15–16]. Copyright © 2016, American Chemical Society.

in **14** it was discovered that the corresponding absorbance occurs in the blue region of the spectrum, providing complementary absorption (Figure 10 c). Because the phenylene rings are not linked together through an uninterrupted conjugation pathway, pendant groups have a smaller overall delocalized π surface, resulting in a peak absorption in the blue region of the spectrum. Through computational analysis, it was determined that the primary source of this absorption was from the Highest Occupied Molecular Orbital + 2 (HOMO-2) to the Lowest Occupied Molecular Orbital (LUMO) (Figure 11 a).

This complementarity allows for panchromatic absorption, where extended conjugation on the Bay axis red-shifts the absorption, while extension of the phenylene region fills in absorption in the smaller wavelengths.

By doing so, compounds such as **16** and **17** can absorb light across the majority of the visible spectrum (Figure 10 d).

Cyclic voltammetry allows for an approximation of the energy levels for the frontier molecular orbitals of the BAI system (Figure 11 b). In the parent BAI molecule **2** a characteristic double reduction, corresponding to an approximate LUMO energy of −3.6 eV, is observed due to reduction of the amide groups. At positive sweep voltages the peak shape often varies between irreversible and pseudoreversible depending on the donor groups, resulting in HOMO levels between −4.9 and −5.5 eV. FMO energy levels determined from cyclic voltammetry were found to be consistent across multiple techniques including ultraviolet

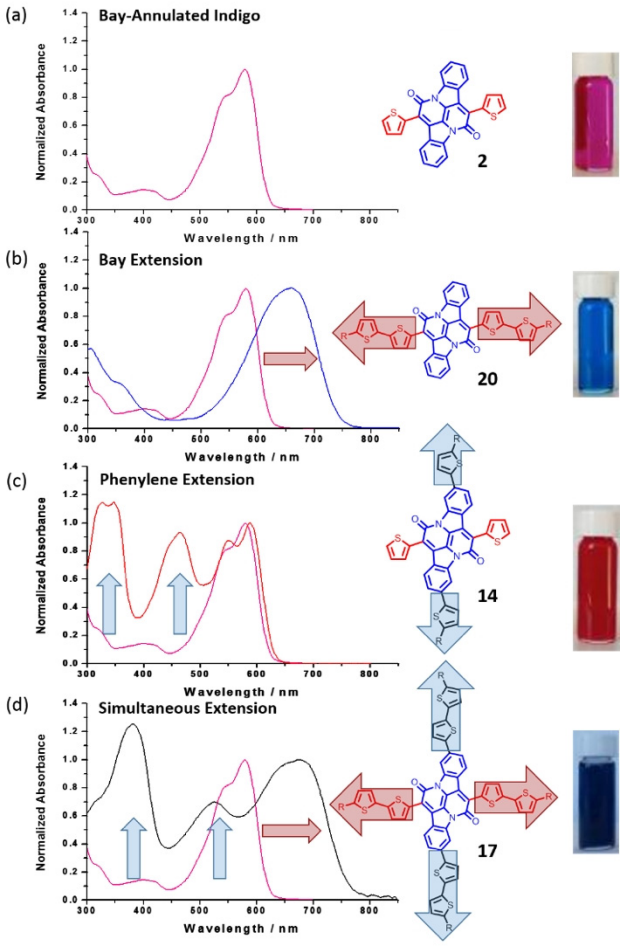

Figure 10. Modulating the absorption profiles of (a) parent BAI **2** by extension of conjugation in the (b) bay direction inducing a red-shift in **20** (c) the phenylene direction to introduce new peaks at lower wavelength in **14**, and (d) both directions simultaneously to provide panchromatic absorption in **17**. Reproduced with permission from references [17]. Copyright © 2016, Royal Society of Chemistry.

photoelectron spectroscopy (UPS) + UV/Vis[15] and photoelectron spectroscopy (PESA) + UV/Vis.[18]

An energy level diagram is given to compare the FMO energies of BAI systems with some benchmark organic semiconductors (Figure 11 c). In comparison with donor systems such as poly-3-hexylthiophene (P3HT, BAI has sufficiently lower HOMO and LUMO to make it energetically compatible for charge transfer (Figure 10 d). When compared to acceptors, BAI have a higher HOMO and LUMO than fullerene based acceptor phenyl-C61-butyric acid methyl ester (PCBM), but approximately equivalent HOMO levels as non-fullerene acceptor (3,9-bis(2-methylene-(3(1,1-dicyanomethylene)indanone))-5,5,11,11-tetrakis(4-hexylphenyl)dithieno[2,3*d*:2′,3′*d*′]indaceno [1,2*b*:5,6*b*′] dithiophene) ITIC.[19]

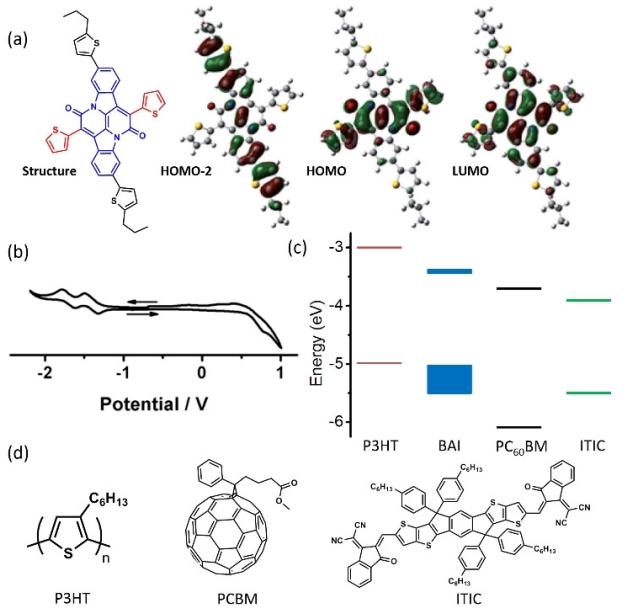

Figure 11. (a) Computational analysis of frontier molecular orbitals (FMOs), (b) cyclic voltammogram of parent BAI molecule **2**. (c) comparison of BAI orbital energy levels with common semiconducting materials with (d) structures shown. Reproduced with permission from references [9,17]. Copyright © 2014, American Chemical Society, Copyright © 2016, Royal Society of Chemistry.

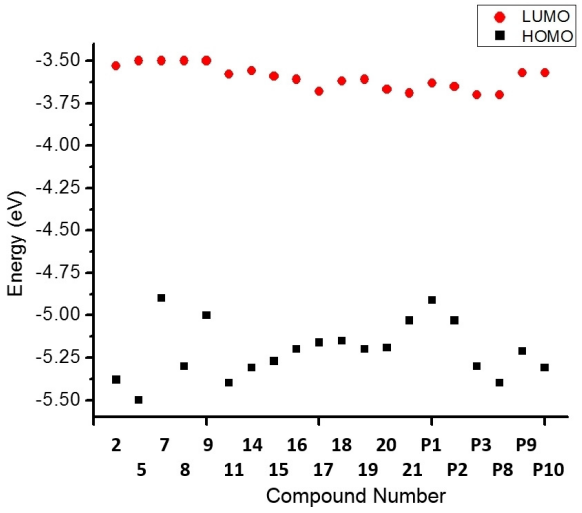

Figure 12. Comparison of electrochemically determined HOMO and LUMO levels of representative BAI compounds.

Computational analysis has shown that the HOMO is localized across the Bay positions through the same conjugation pathway as was shown in Figure 1, whereas the LUMO is more delocalized onto the BAI core. This is consistent with the HOMO being fairly simple to modify by altering the donor groups. The LUMO energy is more consistent due to being tied more intimately to the withdrawing amide functionality. A collection of the FMO energy levels for representative BAI compounds gives a clear visual representation of this trend (Figure 12).

3. Applications

3.1. Organic Field-Effect Transistors

Polymeric BAI materials have shown outstanding semiconducting properties, as summarized in Table 1. They are a member of a fairly limited set of materials capable of ambipolar charge transport with balanced conduction of both electrons and holes, such as PDI and DPP.[20] The electron mobility of 3.11 $cm^2V^{-1}s^{-1}$ displayed in **P14** is among the highest for n-type conducting polymers (entry 12), matched with a respectable hole mobility of 0.63 $cm^2V^{-1}s^{-1}$ (entry 11).[15]

In fact, high ambipolar mobilities are observed in a range of BAI-based polymers. The ambipolar transport behavior is found to be highly dependent on the device fabrication conditions. Using appropriate electrode materials, and/or UV/O_3 treatment, **P14** displays distinctive ambipolar (entry 10), hole enhanced (entry 11) and electron enhanced (entry 12) transport behavior. By choosing a metal with work function similar to the HOMO/conduction band or LUMO/valence band, unipolar devices can lower charge injection barriers leading to lower V_{th} and increases in measured mobility.[22] Improvements for the n-type unipolar devices have been attributed not to the aluminum electrode, but the ethoxylated polyethylenimine (PEIE) electron injection layer.[15]

The ambipolar device behavior is also sensitive to oxygen. While ambipolar under vacuum, in the presence of air several BAI polymers become more hole conductive while electron conductivity decreases (entries 1–4).[9] This is caused by molecular oxygen introduced electron traps that act as a p-type dopant for the polymers.[20] Despite this doping effect, the polymers maintain their semiconducting capacity implying that there is negligible decomposition due to oxidation.

Thermal annealing often increases crystallinity due to relaxation of the polymer into a more thermodynamically stable conformation resulting in improved mobilities. This is demonstrated in the case of **P11** which shows a 6x and 4x fold increase in hole and electron mobility respectively upon increasing annealing temperatures from 100 °C to 190 °C (entries 5, 6).

Moving the branching point of alkyl chains in otherwise identical polymers was conducted to gain insight into structure – function relationships.[18] Polymers **P11**–**P14** have

Table 1. Summarized OFET device characteristics based on BAI polymers.

Entry [ref]	Polymer[a]	Format	Channel	Gate (contact)	Electrode	Anneal	h+ mobility ($cm^2V^{-1}s^{-1}$)	h+ V_{th}	h+ I_{on}/I_{off}	e- mobility ($cm^2V^{-1}s^{-1}$)	e- V_{th}	e- I_{on}/I_{off}
1[9]	**P1**	BG:BC	50:400	SiO_2/OTs	Au/Cr	160 °C	1.5	−6	E3–E4	0.41	50	E1–E2
2[9]	**P1**[b]	BG:BC	50:400	SiO_2/OTs	Au/Cr	160 °C	1.7	−20	E3–E4	–	–	–
3[9]	**P2**	BG:BC	50:400	SiO_2/OTs	Au/Cr	160 °C	1.4	−21	E3	0.09	36	E2
4[21]	**P7**[b]	BG:BC	40:1400	SiO_2/OTs	Au	100 °C	0.39	−3	E3	–	–	–
5[2a,15]	**P11**	TG:BC	40:1000	Al/CYTOP	Al/Au	100 °C	0.04	−120	E4	0.075	43	E5
6[15]	**P11**	TG:BC	40:1000	Al/CYTOP	Al/Au	190 °C	0.25	−99	E1–E2	0.31	99	E1–E2
7[15]	**P12**	TG:BC	40:1000	Al/CYTOP	Al/Au	190 °C	0.16	−119	E1–E2	0.73	108	E2
8[2a,15]	**P13**[d]	TG:BC	40:1000	Al/CYTOP	UV-O_3 Au	190 °C	0.002	−155	E2	–	–	–
9[2a,15]	**P13**[e]	TG:BC	40:1000	Al/CYTOP	Al[c]	190 °C	–	–	–	0.028	89	E3
10[15]	**P14**	TG:BC	40:1000	Al/CYTOP	Al/Au	190 °C	0.2	−133	E1	1.8	115	E2–E3
11[15]	**P14**[d]	TG:BC	40:1000	Al/CYTOP	UV-O_3 Au	190 °C	0.52	−121	E1	–	–	–
12[15]	**P14**[e]	TG:BC	40:1000	Al/CYTOP	Al[c]	190 °C	–	–	–	3.11	74	E4
13[18]	**P15**[d]	TG:BC	40:1000	Al/CYTOP	UV-O_3 Au	190 °C	0.11	−112	E1–E2	–	–	–
14[18]	**P15**[e]	TG:BC	40:1000	Al/CYTOP	Al[c]	190 °C	–	–	–	1.01	79	E4–E5
15[18]	**P16**[d]	TG:BC	40:1000	Al/CYTOP	UV-O_3 Au	190 °C	0.13	−65	E1–E2	–	–	–
16[18]	**P16**[e]	TG:BC	40:1000	Al/CYTOP	Al[c]	190 °C	–	–	–	1.04	54	E4–E5
17[18]	**P18**[d]	TG:BC	40:1000	Al/CYTOP	UV-O_3 Au	190 °C	0.38	−107	E3	–	–	–
18[18]	**P18**[e]	TG:BC	40:1000	Al/CYTOP	Al[c]	190 °C	–	–	–	0.63	88	E4–E5

[a] Measured under vacuum or nitrogen. [b] Measured in air. [c] treated with ethoxylated polyethylenimine. [d] p-type unipolar device. [e] n-type unipolar device.

a branching point relatively close to the polymer backbone making π-π stacking more challenging. Extending the branching point by two carbons in **P15–P18** maintained backbone order while displaying improved π interactions between polymers.

However, this alkyl extension also caused the polymers to lose the largely edge-on lamellar preference of the **P11–P14** species, giving a mixed edge-on and face-on orientation relative to the substrate. In OFETs, a slight decrease in hole mobilities was observed along with a tenfold increase in on/off ratios for n-type devices.

3.2. Organic Photovoltaics

Polymeric bay-annulated indigo materials have shown encouraging results as photovoltaic materials. The high stability, large extinction coefficients, and outstanding conductivity provide a solid platform for development. In initial reports, BAI donor-acceptor polymers have been paired with fullerene based acceptors due to sufficient HOMO and LUMO offsets to drive excitonic charge separation (Figure 10c).[23] Bulk heterojunction active layers are used to provide mixing of the donor and acceptor domains with percolation networks to the electrodes within the exciton diffusion length.

Largely due to deep HOMO levels of the BAI based systems, V_{oc} values for these BAI-PCBM systems are relatively

Table 2. Summary of organic photovoltaic device characteristics based on BAI polymers.

Entry [ref]]	Polymer	BAI : PC[71]BM ratio	Additive	Anneal	Bottom Electrode	Interlayer	Top Electrode	V_{OC}	J_{SC} (mA/cm^2)	FF	PCE
1[9,24]	**P1**	1 : 1	1 % DIO	120 °C	ITO	ZnO nanoparticle	MoO_3/Ag	0.61	6.05	0.5	2.3 %
2[9,24]	**P2**	1 : 1	1 % DIO	120 °C	ITO	ZnO nanoparticle	MoO_3/Ag	0.81	9.01	0.38	2.7 %
3[9,24]	**P3**	1 : 1	1 % DIO	120 °C	ITO	ZnO nanoparticle	MoO_3/Ag	0.83	5.55	0.31	1.4 %
4[26]	**P4**	1 : 4	10 % TCE	85 °C	ITO	PEDOT : PSS	Ca : Al	0.64	5.37	0.36	1.2 %
5[26]	**P5**	1 : 4	–	85 °C	ITO	PEDOT : PSS	Ca : Al	0.82	6.67	0.44	2.4 %
6[26]	**P6**	1 : 4	–	85 °C	ITO	PEDOT : PSS	Ca : Al	0.8	6.83	0.41	2.2 %
7[24]	**P8**	1 : 1	1 % DIO	120 °C	ITO	ZnO nanoparticle	MoO_3/Ag	0.65	7.76	0.53	2.7 %
8[24]	**P9**	1 : 1	1 % DIO	120 °C	ITO	ZnO nanoparticle	MoO_3/Ag	0.85	8.15	0.43	3.0 %
9[24]	**P10**	1 : 1	1 % DIO	120 °C	ITO	ZnO nanoparticle	MoO_3/Ag	0.93	9.23	0.45	3.9 %
10[15]	**P11**	1 : 4	–	–	ITO	PEDOT : PSS	LiF : Al	0.61	10.2	0.66	4.1 %
11[15]	**P12**	1 : 3	–	–	ITO	PEDOT : PSS	LiF : Al	0.57	10.3	0.6	3.5 %
12[15]	**P13**	1 : 2	–	–	ITO	PEDOT : PSS	LiF : Al	0.69	6	0.43	1.8 %
13[15]	**P14**	1 : 2	–	–	ITO	PEDOT : PSS	LiF : Al	0.57	4.4	0.53	1.3 %

high for low bandgap materials. Devices with moderate PCEs of 4.1 % and 3.9 % have been independently fabricated which show promise, but also suggest that there are challenges for BAI materials to overcome (Table 2).[15] In particular, the J_{sc} and FF in all cases are lower than desired and need to be improved. A likely culprit is the phase separation of both BAI and fullerene materials.

Alkylation of polymers is a common strategy to modify phase morphology, however a fine balance has to be carefully maintained for ideal crystallinity and phase separation. Polymers without bulky sidechains to prevent aggregation can cause the polymer to be excessively crystalline. This crystallinity impedes proper mixing of the donor and acceptor species, resulting in inferior domains and inefficient charge transport. This is clear with **P14**, which shows high crystallinity and outstanding OFET properties, but displays poor OPV performance due to insufficient mixing with the fullerene acceptor (entry 13).

On the other hand, when monomers are equipped with excessively large alkyl chains, the polymers tend to lack sufficient crystallinity resulting in amorphous active layers unsuitable for charge transport. Understanding and improving the phase morphology is thus crucial for improving the efficiencies of these devices.

To understand how alkyl chain placement on BAI monomers effects OPV performance, polymers **P8–P10** were equipped with 2-ethylhexyl ether sidechains on the phenylene positions, to replace the 3-dodecylthiophene solubilizing groups in **P1–P3**.[24]

The resulting polymers showed decreased crystallinity compared to **P1–P3**, commensurate with increased phase mixing with acceptor domains. The resulting devices showed improved V_{oc}, fill factor (FF), and power conversion efficiency (PCE) and improved J_{sc} for **P8** and **P10** (entries 1–3, 7–9). Nevertheless, GIWAXS, low J_{sc}, and FF suggest that further improvement in phase morphology is necessary for better efficiency.

BAI based materials have also been used as additives in tertiary solar cells (Figure 13). In both examples, P3HT was selected as the primary donor polymer and PCBM as the primary acceptor.[21,25] Due to the intermediate energy level alignment between these two species, BAI derivatives can act as a mediator for charge transfer between the donor and acceptor.

In contrast to solvent additives, these BAI based additives remain in the film and provide additional absorption. Because of the large π-surface area of BAI materials, only small percentages are necessary in order to strongly interact with other species in the active layer. However, at high loadings, the crystallinity of BAI causes self-aggregation, disrupting the film morphology. Both reported systems including BAI as additives in small percentages have improved the performance of traditional P3HT : PC60BM devices, 4.1 % PCE for **9** and 3.8 % PCE for **P7**. New developments in the area of NFAs may provide an alternative to the highly crystalline fullerene acceptors, opening up new directions to improve performance.

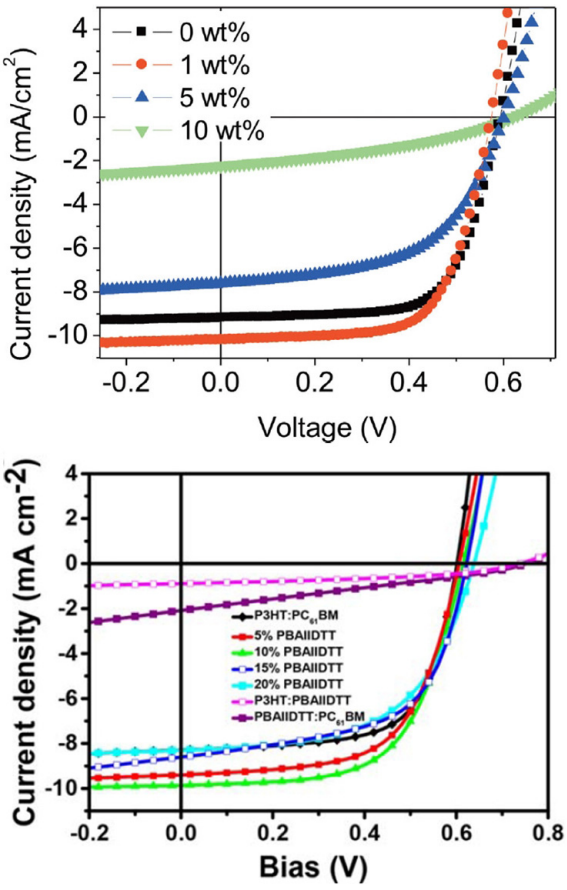

Figure 13. J–V curves for Tertiary OPV devices using P3HT as a donor, PCBM as an acceptor and BAI compounds (a) **25**, and (b) **P7** as additives. Reproduced with permission from references [21,25]. Copyright © 2018, John Wiley and Sons.

BAI-based molecule **22** has been utilized as the light absorber in dye-sensitized solar cells (DSSC).[27] However, it was noted that a lack of spacial separation of charges within the BAI small molecule may increase charge recombination and can lower device performance. This calls for more molecular-level structural tuning for further efficiency improvement.

3.3. Electrochromic Devices

BAI polymers have also been utilized in less conventional applications such as electrochromic devices. Electrochromism, the ability of a material's color to be influenced by a voltage potential, has been utilized in a number of commercial applications, notably shading and color control of windows. Due to the introduction of charged states, air oxidation, and degradation from water, stability is a considerable challenge for most electrochromic materials. Polymers **P9** and **P10** were tested for electrochromic capacity and found to be very robust, successfully cycling 7500 times before degradation under ambient conditions,[16] and in the case of **P9**, high optical contrast of 41 % and 59 % were achieved for visible and IR regions, respectively (Figure 14). The stability is attributed to significant stabilization of the polymer polarons (radical cation) and bipolarons (dication), generated under oxidative biases, through nitrogen resonance from the carbazole co-monomer. Additionally, the BAI monomer can stabilize the charge by maintaining conjugation through the polymer in the charged state.

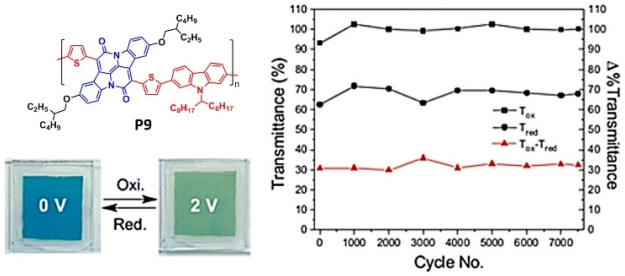

Figure 14. An air-stable electrochromic device based on **P6** showing both oxidized and reduced forms, as well as cycling stability. Reproduced with permission from reference [16]. Copyright © 2016, American Chemical Society.

3.4. Photoacoustic Molecular Imaging

The high absorption of BAI polymers in the near-IR range of the visible spectrum has also rendered them viable materials for bioimaging applications. Because hemoglobin and water have low absorption in the 620–920 nm range, there is a particular interest in utilizing chromophores that absorb light within this "optical window" for bioimaging. By encapsulating **P14** in a micelle with the lipid, 1,2-dipalmitoyl-sn-glycero-3-phosphocholine (DPPC), the polymer can be made "hydrophilic" while also protecting it from light-induced biological degradation (Figure 15).[28] No adverse toxicity effects were observed when the micelle was incubated in a 293T human embryonic kidney cell line MTt assay. These particles have an exceptional extinction coefficient, making them an order of magnitude more absorbent than recently published examples.[29] Additionally, laser excitation studies of these particles showed remarkable stability with no visible degradation up to 2×10^4 pulses at wavelengths between 700–800 nm at a fluence of ~2 mJ cm^{-2}. These particles were employed for *in vivo* photoacoustic imaging studies, where laser excitation of the chromophoric species generates an ultrasound image that can be recorded with high spacial resolution. In mouse studies the encapsulated BAI polymers showed high contrast from the surrounding biological matrix.

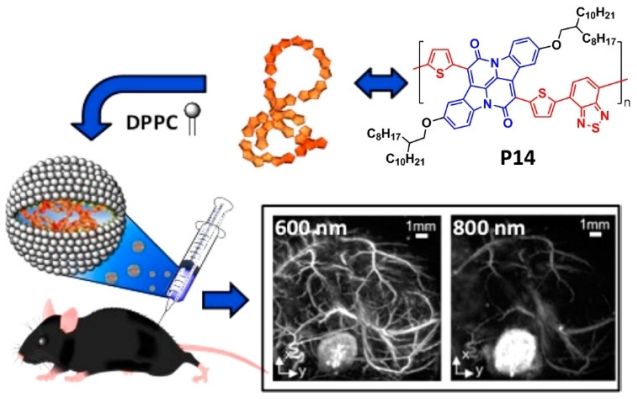

Figure 15. Utilization of lipid encapsulated **P14** nanoparticles for photoacoustic imaging. Figure includes image of an injected tumor taken using 600 nm excitation (left) with background noise from biological sources alongside an image using excitation at 800 nm (right) with injected tumor visible. Reproduced with permission from reference [28]. Copyright © 2017, American Chemical Society.

3. Summary and Outlook

The ability to synthesize diverse materials from simple and inexpensive starting materials through straightforward transformations makes BAI a great building block for semiconductor development. Overall BAI-based materials show promising performance in a number of organic semiconductor applications due to stability, high absorbance ($\varepsilon = 10^5$) into the near IR region, and fine control over both electronics and physical properties through choice of bay-annulation and monomer. Record ambipolar conductivity is made possible through an unusually ordered yet nonplanar polymer backbone.

However, there are still many areas to explore in this area of research. One of the major challenges facing BAI materials for OPV applications is to realize good active layer morphologies. This can potentially be addressed through modification of sidechains and careful optimization of device fabrication.

Non-fullerene acceptors (NFA) have emerged as an alternative to traditional fullerene based electron acceptors.[30] Many NFAs such as ITIC possess HOMO levels very similar to the BAI polymers, and may be too energetically similar to effect charge separation. However, as more NFA species are becoming available with deeper HOMOs, BAI materials may yet overcome these problems. Additionally, the high HOMO levels of BAI molecules and polymers make them particularly well suited for high V_{oc} applications. Although BAI OPVs have shown promising results, there is much room for improvement, particularly in synthesizing novel polymers with improved active layer phase morphology.

Due to the high HOMO and LUMO levels of the BAI system, it has exclusively been used as a donor in OPV. In order to provide use as an acceptor material a number of strategies can be utilized. A fluorination approach has been successfully applied in many cases to lower the frontier molecular orbitals but often comes with additional benefits such as improved charge transport, and improved intermolecular interactions.[31] Alternatively, the addition of secondary acceptor groups on the bay position could lower the LUMO to make the overall molecule or polymer electron accepting.

By taking advantage of the complementary absorption in molecules with aryl substitution at the phenylene position, EQE and J_{sc} could be greatly increased. This strategy for increasing adsorption has been wholly underutilized and could have a large impact on device performance.

Finally, desymmetrized BAI units have untapped potential, for the synthesis of new semiconductors and electroactive supramolecular structures. DSSC could potentially benefit from a desymmetrized BAI molecule with additional sidechain engineering to increase loadings. Molecular wires based on **9** and Langmuir-Blodgett films of amphiphilic **6** are currently being investigated, but there is significantly more room for exploration.

Acknowledgements

This work was conducted at the Molecular Foundry and was supported by the Office of Science, Office of Basic Energy Sciences, of the U.S. Department of Energy under Contract No. DE-AC02-05CH11231.

References

[1] a) A. Facchetti, *Nat. Mater.* **2013**, *12*, 598; b) T. W. Kelley, P. F. Baude, C. Gerlach, D. E. Ender, D. Muyres, M. A. Haase, D. E. Vogel, S. D. Theiss, *Chem. Mater.* **2004**, *16*, 4413–4422.

[2] a) K. Takimiya, I. Osaka, M. Nakano, *Chem. Mater.* **2014**, *26*, 587–593; b) Z. G. Zhang, J. Wang, *J. Mater. Chem.* **2012**, *22*, 4178–4187; c) P. M. Beaujuge, J. M. J. Fréchet, *J. Am. Chem. Soc.* **2011**, *133*, 20009–20029; d) Y. Lin, X. Zhan, *Acc. Chem. Res.* **2016**, *49*, 175–183.

[3] a) L. Dou, J. Gao, E. Richard, J. You, C.-C. Chen, K. C. Cha, Y. He, G. Li, Y. Yang, *J. Am. Chem. Soc.* **2012**, *134*, 10071–10079; b) J. C. Bijleveld, A. P. Zoombelt, S. G. J. Mathijssen, M. M. Wienk, M. Turbiez, D. M. de Leeuw, R. A. J. Janssen, *J. Am. Chem. Soc.* **2009**, *131*, 16616–16617.

[4] a) W. Cui, J. Yuen, F. Wudl, *Macromolecules* **2011**, *44*, 7869–7873; b) S. M. McAfee, J. M. Topple, J.-P. Sun, I. G. Hill, G. C. Welch, *RSC Adv.* **2015**, *5*, 80098–80109.

[5] E. Steingruber, in *Ullmann's Encyclopedia of Industrial Chemistry*, Wiley-VCH Verlag GmbH & Co. KGaA, **2000**.

[6] S. Yamazaki, A. L. Sobolewski, W. Domcke, *Phys. Chem. Chem. Phys.* **2011**, *13*, 1618–1628.

[7] a) M. Irimia-Vladu, E. D. Głowacki, P. A. Troshin, G. Schwabegger, L. Leonat, D. K. Susarova, O. Krystal, M. Ullah, Y. Kanbur, M. A. Bodea, V. F. Razumov, H. Sitter, S. Bauer, N. S. Sariciftci, *Adv. Mater.* **2012**, *24*, 375–380; b) C. Guo, J. Quinn, B. Sun, Y. Li, *J. Mater. Chem. C,* **2015**, *3*, 5226–5232.
[8] a) G. Engi, *Angew. Chem.* **1914**, *27*, 144–148; b) T. Posner, E. Wallis, *Ber. Dtsch. Chem. Ges. A and B* **1924**, *57*, 1673–1681; c) C. Simon, in *The Chemical Industry in Europe, 1850–1914: Industrial Growth, Pollution, and Professionalization* (Eds.: E. Homburg, A. S. Travis, H. G. Schröter), Springer Netherlands, Dordrecht, **1998**, pp. 9–27; d) J. Seixas de Melo, R. Rondão, H. D. Burrows, M. J. Melo, S. Navaratnam, R. Edge, G. Voss, *J. Phys. Chem. A*, **2006**, *110*, 13653–13661.
[9] B. He, A. B. Pun, D. Zherebetskyy, Y. Liu, F. Liu, L. M. Klivansky, A. M. McGough, B. A. Zhang, K. Lo, T. P. Russell, L. Wang, Y. Liu, *J. Am. Chem. Soc.* **2014**, *136*, 15093–15101.
[10] M. A. Kolaczkowski, B. He, Y. Liu, *Org. Lett.* **2016**, *18*, 5224–5227.
[11] a) K. J. Fallon, N. Wijeyasinghe, N. Yaacobi-Gross, R. S. Ashraf, D. M. E. Freeman, R. G. Palgrave, M. Al-Hashimi, T. J. Marks, I. McCulloch, T. D. Anthopoulos, H. Bronstein, *Macromolecules* **2015**, *48*, 5148–5154; b) A. Baeyer, V. Drewsen, *Ber. Dtsch. Chem. Ges.* **1882**, *15*, 2856–2864.
[12] B. X. ■■**surname**■■, Q. Ren, M. A. Kolaczkowski, C. Sun, C. Ou, Y. Sun, L. Xie, W. Huang, *Dyes Pigm.* **2019**, *160*, 25–27.
[13] J. Y. Back, T. K. An, Y. R. Cheon, H. Cha, J. Jang, Y. Kim, Y. Baek, D. S. Chung, S.-K. Kwon, C. E. Park, Y.-H. Kim, *ACS Appl. Mater. Interfaces* **2015**, *7*, 351–358.
[14] T. Furuyama, D. Tamura, H. Maeda, M. Segi, *Tetrahedron Lett.* **2018**, *59*, 2913–2916.
[15] K. J. Fallon, N. Wijeyasinghe, E. F. Manley, S. D. Dimitrov, S. A. Yousaf, R. S. Ashraf, W. Duffy, A. A. Y. Guilbert, D. M. E. Freeman, M. Al-Hashimi, J. Nelson, J. R. Durrant, L. X. Chen, I. McCulloch, T. J. Marks, T. M. Clarke, T. D. Anthopoulos, H. Bronstein, *Chem. Mater.* **2016**, *28*, 8366–8378.
[16] B. He, W. T. Neo, T. L. Chen, L. M. Klivansky, H. Wang, T. Tan, S. J. Teat, J. Xu, Y. Liu, *ACS Sustainable Chem. Eng.* **2016**, *4*, 2797–2805.
[17] B. He, D. Zherebetskyy, H. Wang, M. A. Kolaczkowski, L. M. Klivansky, T. Tan, L. Wang, Y. Liu, *Chem. Sci.* **2016**, *7*, 3857–3861.
[18] K. J. Fallon, A. Santala, N. Wijeyasinghe, E. F. Manley, N. Goodeal, A. Leventis, D. M. E. Freeman, M. Al-Hashimi, L. X. Chen, T. J. Marks, T. D. Anthopoulos, H. Bronstein, *Adv. Funct. Mater.* **2017**, *27*, 1704069.
[19] Y. Lin, J. Wang, Z.-G. Zhang, H. Bai, Y. Li, D. Zhu, X. Zhan, *Adv. Mater.* **2015**, *27*, 1170–1174.
[20] Y. Zhao, Y. Guo, Y. Liu, *Adv. Mater.* **2013**, *25*, 5372–5391.
[21] J. Zhu, T. Li, K. Shi, J. Wang, Y. Lin, G. Yu, X. Zhan, *J. Polym. Sci. Part A* **2018**, *56*, 213–220.
[22] S. Rentenberger, A. Vollmer, E. Zojer, R. Schennach, N. Koch, *J. Appl. Phys.* **2006**, *100*, 053701.
[23] a) H.-W. Li, Z. Guan, Y. Cheng, T. Lui, Q. Yang, C.-S. Lee, S. Chen, S.-W. Tsang, *Adv. Electron. Mater.* **2016**, *2*, 1600200; b) M. Knupfer, *Appl. Phys. A.* **2003**, *77*, 623–626.
[24] B. K. ■■**surname**■■, L. M. He, T. L. Chen, A. B. Pun, B. Yang, M. A. Koalczkowski, R. Lu, Y. Liu, *Unpublished Results* **2018**.
[25] B. Yang, M. A. Kolaczkowski, M. A. Brady, J. K. Keum, J. F. Browning, T. L. Chen, Y. Liu, *Solar RRL* **2018**, *2*, 1700208.
[26] J. Brebels, K. C. C. W. S. Klider, M. Kelchtermans, P. Verstappen, M. Van Landeghem, S. Van Doorslaer, E. Goovaerts, J. R. Garcia, J. Manca, L. Lutsen, D. Vanderzande, W. Maes, *Org. Electron.* **2017**, *50*, 264–272.
[27] G. H. Summers, E. A. Gibson, *ChemPhotoChem* **2018**, *2*, 498–506.
[28] T. Stahl, R. Bofinger, I. Lam, K. J. Fallon, P. Johnson, O. Ogunlade, V. Vassileva, R. B. Pedley, P. C. Beard, H. C. Hailes, H. Bronstein, A. B. Tabor, *Bioconjugate Chem.* **2017**, *28*, 1734–1740.
[29] K. Pu, J. Mei, J. V. Jokerst, G. Hong, A. L. Antaris, N. Chattopadhyay, A. J. Shuhendler, T. Kurosawa, Y. Zhou, S. S. Gambhir, Z. Bao, J. Rao, *Adv. Mater.* **2015**, *27*, 5184–5190.
[30] a) P. Cheng, G. Li, X. Zhan, Y. Yang, *Nat. Photonics* **2018**, *12*, 131–142; b) W. Chen, Q. Zhang, *J. Mater. Chem. C,* **2017**, *5*, 1275–1302; c) C. Yan, S. Barlow, Z. Wang, H. Yan, A. K. Y. Jen, S. R. Marder, X. Zhan, *Nat. Rev. Mater.* **2018**, *3*, 18003.
[31] a) Q. Zhang, M. A. Kelly, N. Bauer, W. You, *Acc. Chem. Res.* **2017**, *50*, 2401–2409; b) K. Kranthiraja, D. X. Long, V. G. Sree, W. Cho, Y.-R. Cho, A. Zaheer, J.-C. Lee, Y.-Y. Noh, S.-H. Jin, *Macromolecules* **2018**, *51*, 5530–5536.

Manuscript received: September 16, 2018
Revised manuscript received: December 14, 2018
Accepted: December 20, 2018
Version of record online: ■■ ■■, ■■■■

PERSONAL ACCOUNT

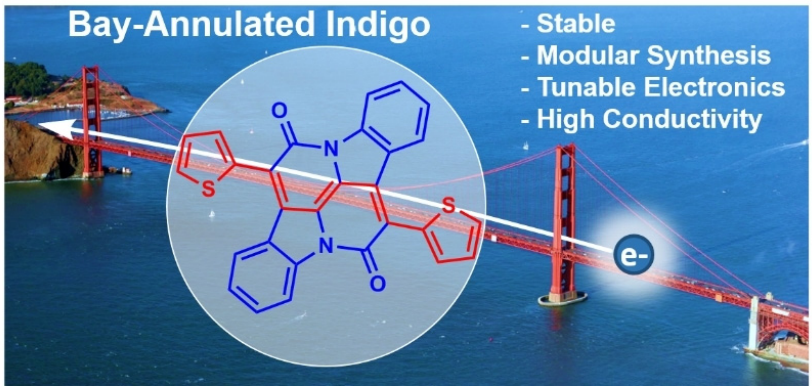

■■■Dear Author, please provide a TOC text (about three short sentences, which summarize the content of your article). This text will appear together with the TOC figure on the first pages of the online issue, if your article will become part of this issue.■■■

*M. A. Kolaczkowski, Dr. Y. Liu**